# Application of the numerical model of temperature-dependent thermal conductivity in Ca$_{1-x}$Y$_x$F$_{2+x}$ heterovalent solid solution nanocomposites

Pavel A. Popov[1], Alexandr V. Shchelokov[1], Vasilii A. Konyushkin[2], Andrey N. Nakladov[2], Pavel P. Fedorov[2]

[1]Petrovsky Bryansk State University, Bryansk, Russia

[2]Prokhorov General Physics Institute of the Russian Academy of Sciences, Moscow, Russia

Corresponding author: Pavel P. Fedorov, ppfedorov@yandex.ru

ABSTRACT A series of Ca$_{1-x}$Y$_x$F$_{2+x}$ solid solution $x = 0.0005, 0.003, 0.007, 0.013, 0.02, 0.03, 0.04$ single crystals were grown using the Bridgman method. The thermal conductivity of single crystals was measured using the absolute method of longitudinal heat flow in the range of $50 - 300$ K. With an increase in the concentration of yttrium fluoride in the solid solution, a transition is observed from the temperature dependence characteristic of single crystals to a monotonically increasing one with increasing temperature, which is characteristic of disordered media. This behavior is associated with the scattering of phonons on nanosized clusters of defects present in the solid solution. Within the framework of a two-component model, including a superposition of thermal resistance coefficients from ordered and disordered media, a system of equations was obtained that provides a quantitative description of the experiment.

KEYWORDS nanocomposite, inorganic fluorides, fluorite, thermal conductivity, phase diagram, heterovalent isomorphism, defect clusters

FOR CITATION Popov P.A., Shchelokov A.V., Konyushkin V.A., Nakladov A.N., Fedorov P.P. Application of the numerical model of temperature-dependent thermal conductivity in Ca$_{1-x}$Y$_x$F$_{2+x}$ heterovalent solid solution nanocomposites. *Nanosystems: Phys. Chem. Math.*, 2025, **16** (1), 67–73.

## 1. Introduction

Solid solutions of yttrium fluoride in calcium fluoride are a classical object of solid state physics and chemistry. The mineral yttrofluorite was discovered more than 100 years ago [1, 2], its research made it possible to formulate the concept of heterovalent isomorphism [3–5]. Further studies of the structure of the Ca$_{1-x}$Y$_x$F$_{2+x}$ solid solution [6–22] revealed a complex pattern of association of structural defects, leading to the formation of nanosized clusters coherently embedded in the fluorite lattice [23–25]. This allows us to consider the corresponding solid solution as a unique example of nanosized composites [26, 27].

The phase diagram of the CaF$_2$–YF$_3$ system is presented in Fig. 1 [28]. The Ca$_{1-x}$Y$_x$F$_{2+x}$ solid solution is characterized by closeness of the liquidus and solidus curves, which makes it possible to grow high-quality single crystals from the melt [29]. The low-temperature decomposition of this solid solution is inhibited.

The Ca$_{1-x}$Y$_x$F$_{2+x}$ solid solution is a photonics material, transparent in a wide optical range, from vacuum ultraviolet to mid-IR, differing from pure fluorite in its increased hardness and lack of cleavage [25]. It is a matrix for solid-state lasers, both in the form of single crystals and ceramics [30–51]. In addition, it is characterized by increased ionic conductivity, which determines its use in electrochemical studies [52–54].

Thermal conductivity is the main characteristic that determines the behavior of a material under operating conditions. Preliminary measurements of the thermal conductivity of some single crystals of the Ca$_{1-x}$Y$_x$F$_{2+x}$ solid solution were carried out in [55, 56]. Currently, a model has emerged [57], based on the approach formulated in [58, 59], which makes it possible to quantitatively describe the temperature and concentration dependences of the thermal conductivity of such solid solutions.

The purpose of this work was to determine the thermal conductivity of original nanocomposite system, namely, single crystals of the Ca$_{1-x}$Y$_x$F$_{2+x}$ solid solution for the missing concentration region and to quantitatively describe the experimental results based on the existing model.

The technique for growing crystals is identical to that used in [56]. The starting materials used were yttrium fluoride of the chemically pure grade, melted under a fluorinating atmosphere of Teflon pyrolysis products, and calcium fluoride – broken optical crystals produced by the State Optical Institute named after S. I. Vavilov. Single crystals with a diameter of 10 mm were grown by the Bridgman method in a seven-channel graphite crucible in a static CF$_4$ atmosphere (pressure 80 Torr). Drawing speed is 10 mm/h, temperature gradient is $50 \pm 10$ K/cm. No corrections were made for changes in composition during crystal growth.
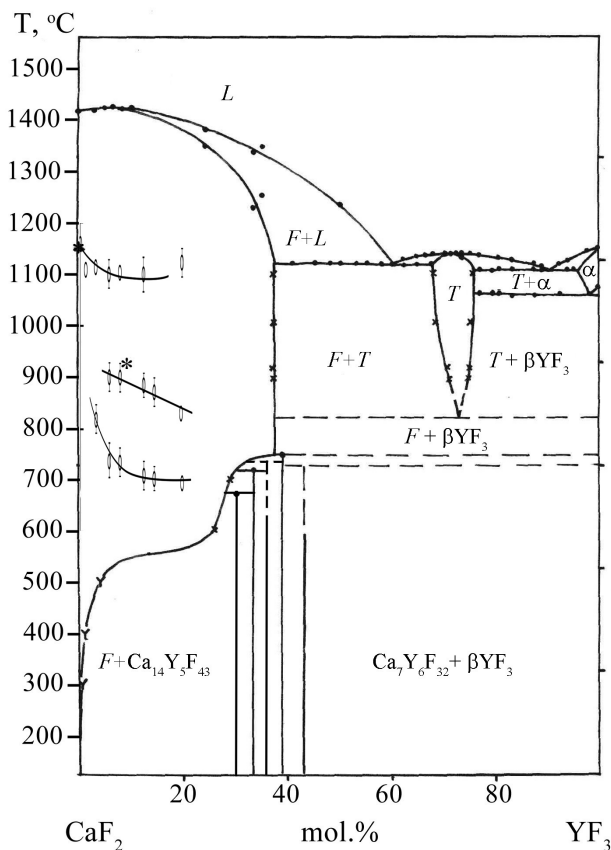
FIG. 1. Phase diagram of the $CaF_2$–$YF_3$ system [28]. Phase $F$ denotes the $Ca_{1-x}Y_xF_{2+x}$ solid solution

The objects of the experimental study of thermal conductivity in this work were single-crystal samples of $Ca_{1-x}Y_xF_{2+x}$ with yttrium trifluoride content $x = 0.0005, 0.003, 0.007, 0.013, 0.02, 0.03, 0.04$ cubic structure.

The determination of thermal conductivity in the temperature range 50 – 300 K was carried out using the absolute stationary method of longitudinal heat flow [60]. The error in determining the absolute value of thermal conductivity did not exceed 5 %.

The measurement results in the form of graphs of the temperature dependence of thermal conductivity $k(T)$ are presented in Fig. 2. To complete the picture, the results of previous studies of the thermal conductivity of $Ca_{1-x}Y_xF_{2+x}$ samples with the content of the second component $x = 0.005$ and $x = 0.05 - 0.20$ have been added here (the technique for synthesizing single crystals and measuring thermal conductivity is identical to those used in this work) [56]. The numerical data $k(T)$ for the new samples studied are given in Table 1.

TABLE 1. Smoothed values of thermal conductivity of $Ca_{1-x}Y_xF_{2+x}$ single crystals

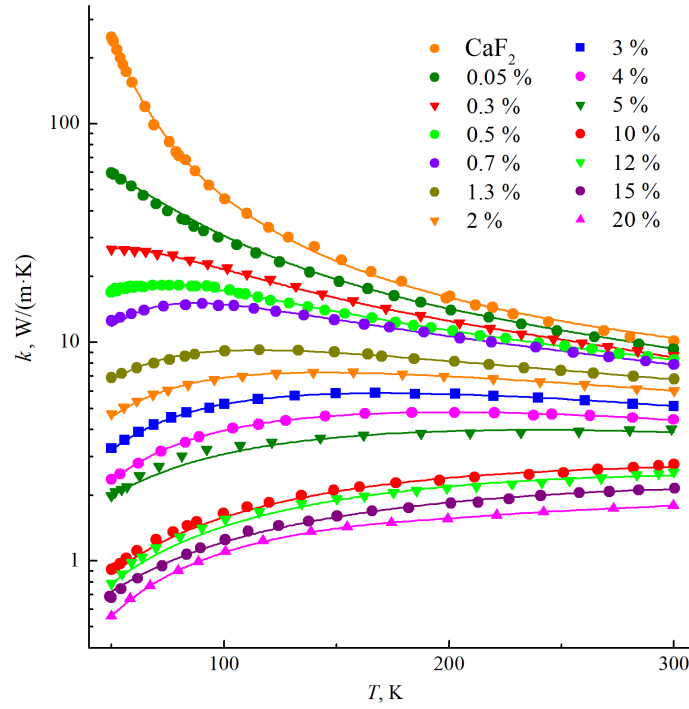| YF$_3$ Content, mol. % | Temperature, K | | | | | |
|---|---|---|---|---|---|---|
| | 50 | 100 | 150 | 200 | 250 | 300 |
| 0.05 | 59.5 | 29.5 | 19.2 | 14.2 | 11.2 | 9.3 |
| 0.3 | 26.7 | 21.9 | 16.1 | 12.5 | 10.2 | 8.7 |
| 0.7 | 12.5 | 14.8 | 12.7 | 10.7 | 9.2 | 7.9 |
| 1.3 | 6.90 | 9.14 | 9.02 | 8.20 | 7.43 | 6.8 |
| 2 | 4.70 | 6.85 | 7.30 | 6.97 | 6.53 | 6.0 |
| 3 | 3.27 | 5.20 | 5.82 | 5.78 | 5.51 | 5.1 |
| 4 | 2.36 | 3.93 | 4.65 | 4.80 | 4.64 | 4.45 |

FIG. 2. Temperature-dependent thermal conductivity coefficient for $Ca_{1-x}Y_xF_{2+x}$ solid solution single crystals: markers represent experimental values, and lines are fitted curves calculated by model (1)

As can be seen in Fig. 2, there is a monotonic concentration transition of the nature of the temperature dependence from typical for dielectric single crystals to glass-like. The low-temperature maximum $k(T)$ inherent in ordered media appears ($x = 0.005$, i.e. 0.5 mol %) in the temperature range studied, becomes lower and wider with increasing concentration, shifts towards higher temperatures and completely disappears at $x > 0.05$. This kind of transition has been detected many times for various heterovalent solid solutions of the $M_{1-x}R_xF_{2+x}$ type, where M = Ca, Sr, Ba, Cd, Pb, R=Y, La–Lu (see, for example, [61–63]). It is associated with the formation of nanosize defect clusters in such crystals and corresponding high-intensity phonon scattering.

The $Ca_{1-x}Y_xF_{2+x}$ solid solution is structurally a model for similar compositions with fluorides of rare earth elements of the yttrium subgroup. The most likely type of defect clusters is the so-called hexameric cluster $Y_6F_{37}$, existing in ordered fluorite-like phases, formed in the system $CaF_2$–$YF_3$ [24,64–66]. This point of view is confirmed by the results of precision structural studies of $Ca_{1-x}Y_xF_{2+x}$ solid solution [17,18,20,21] and investigation of its physical properties [22, 67]. The scheme of embedding such a cluster into the fluorite lattice according to the Bevan, Greis and Strahle [23] model is shown in Fig. 3. The size of such clusters with their defective periphery is about 1.5 nm.
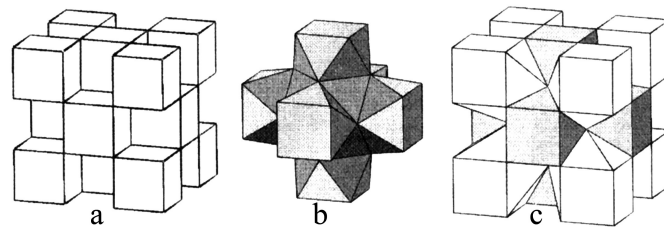


FIG. 3. Fragment of the fluorite lattice (a), the $Y_6F_{37}$ cluster (b), and the $Y_6F_{37}$ cluster incorporated into the fluorite lattice (c)

In application to the obtained experimental values of $k(T)$, we test the relatively simple formulaic expression proposed in [57] for describing the specific thermal resistance $w = 1/k$ of heterovalent solid solutions. This expression looks like:

$$\frac{1}{k} = \frac{1 - A}{\beta\sqrt{\frac{k_0}{d}} \cdot \arctan\left(\frac{\sqrt{k_0}d}{\beta}\right)} + \frac{A}{D + BT + CT^2}. \tag{1}$$

Here $A$ is the contribution of the thermal resistance associated with the introduction of trivalent rare earth ions and the formation of clusters of defects ("amorphous component"); $\beta$ is a parameter depending on the type of rare earth dopant; $k_0$ is the thermal conductivity coefficient of the undoped crystal; $d$ is the concentration of the rare earth dopant; $D$, $B$ and $C$ are coefficients of the polynomial describing the "amorphous component" of the thermal conductivity coefficient.

In this work, the coefficient $k_0$ for the thermal conductivity of a nominally pure $CaF_2$ crystal [68] is taken in accordance with the following expression

$$k_0 = a_1 + a_2 \exp(a_3/T) \, T^{-1}. \tag{2}$$

As can be seen in Fig. 1, the calculated curves have a slight deviation from the experimental $k(T)$ points. The discrepancy in almost all cases does not exceed the experimental error of 5 %. The values of the parameters included in expressions (1) and (2), which do not depend on the concentration of the solid solution, were: $a_1 = 3.38$ W·m$^{-1}$K$^{-1}$, $a_2 = 1499$ W·m$^{-1}$, $a_3 = 104.7$, $\beta = 0.24$. The values of parameters $A$, $B$, $C$ and $D$, directly related to the concentration of yttrium fluoride in the solid solution, are given in Table 2.

TABLE 2. Values of parameters $A$, $B$, $C$ and $D$ included in expression (1)

| YF$_3$ Content, mol. % | $A$ | $C$, W·m$^{-1}$K$^{-3}$ | $B$, W·m$^{-1}$K$^{-2}$ | $D$, W·m$^{-1}$K$^{-1}$ |
|---|---|---|---|---|
| 0.0005 | 0.11 | $-1.183 \cdot 10^{-4}$ | $2.490 \cdot 10^{-2}$ | 8.758 |
| 0.003 | 0.155 | $-2.852 \cdot 10^{-4}$ | $1.036 \cdot 10^{-1}$ | 1.137 |
| 0.005 | 0.17 | $-2.132 \cdot 10^{-4}$ | $9.288 \cdot 10^{-2}$ | $-0.506$ |
| 0.007 | 0.21 | $-2.514 \cdot 10^{-4}$ | $1.087 \cdot 10^{-1}$ | $-1.881$ |
| 0.01 | 0.25 | $-3.868 \cdot 10^{-4}$ | $1.267 \cdot 10^{-1}$ | $-2.983$ |
| 0.013 | 0.30 | $-1.110 \cdot 10^{-4}$ | $5.686 \cdot 10^{-2}$ | $-0.326$ |
| 0.02 | 0.40 | $-1.009 \cdot 10^{-4}$ | $5.154 \cdot 10^{-2}$ | $-0.362$ |
| 0.03 | 0.48 | $-8.767 \cdot 10^{-5}$ | $4.398 \cdot 10^{-2}$ | $-0.347$ |
| 0.04 | 0.55 | $-6.741 \cdot 10^{-5}$ | $3.496 \cdot 10^{-2}$ | $-0.244$ |
| 0.05 | 0.60 | $-4.006 \cdot 10^{-5}$ | $2.355 \cdot 10^{-2}$ | 0.149 |
| 0.1 | 0.68 | $-1.807 \cdot 10^{-5}$ | $1.378 \cdot 10^{-2}$ | $-0.041$ |
| 0.12 | 0.70 | $-1.728 \cdot 10^{-5}$ | $1.288 \cdot 10^{-2}$ | $-0.038$ |
| 0.15 | 0.75 | $-1.288 \cdot 10^{-5}$ | $1.021 \cdot 10^{-2}$ | 0.071 |
| 0.2 | 0.77 | $-1.638 \cdot 10^{-5}$ | $1.032 \cdot 10^{-2}$ | $-0.014$ |

An increase in the concentration of the solid solution is accompanied by a natural increase in the values of parameter $A$ and their approach to the upper threshold value $A = 1$ (see Fig. 4). To some approximation, the dependence $A(d)$, as in the case of the $Ca_{1-x}Yb_xF_{2+x}$ solid solution [57], can be described by a logarithmic function with a constant component (the parameter $d$ in expression (1) is equal to the value $x$ in the composition formula).

It is not possible to detect clear correlations for parameters $B$, $C$ and $D$. To a rough approximation, the decreasing nature of the absolute values of the parameters $C$ and $B$ with increasing Y content, and the weak dependence of $B(d)$ are violated in the region of the lowest concentrations, apparently due to the strong local concentration dependence of the thermal conductivity coefficient. In Fig. 5, this dependence is presented in the form of two isotherms $k(x)$. It can be seen that the new experimental points $k(x)$ for samples with low concentrations fell almost on the interpolation curves proposed earlier [56].

## 2. Conclusion

In the temperature range 50 – 300 K, the thermal conductivity of the original nanocomposite system, namely, single crystals of the $Ca_{1-x}Y_xF_{2+x}$ solid solution with a low concentration of yttrium fluoride ($x = 0.0005 - 0.04$) was experimentally studied. The inclusion of nanosized clusters in the fluorite lattice leads to a sharp drop in thermal conductivity due to pronounced phonon scattering. We proposed the formula expression for the thermal conductivity coefficient. Testing showed its suitability for describing the dependence of the thermal conductivity coefficient on temperature and concentration for heterovalent $Ca_{1-x}R_xF_{2+x}$ solid solutions, where R is represented by Y and Yb, which differ greatly in mass. In the future, it is planned to search for ways to improve the proposed model based on its application to solid solutions of different compositions with a heterovalent type of ion substitution.
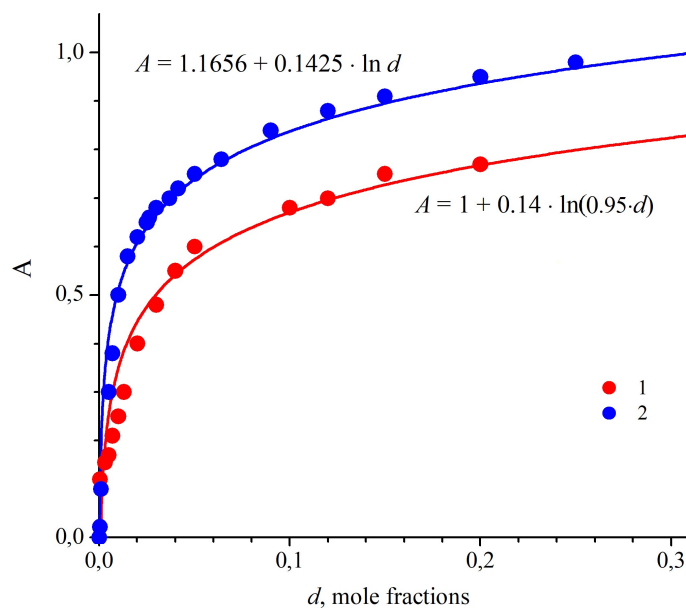
$$A = 1.1656 + 0.1425 \cdot \ln d$$

$$A = 1 + 0.14 \cdot \ln(0.95 \cdot d)$$

FIG. 4. Parameter $A$ versus $YF_3$ concentration in $Ca_{1-x}Y_xF_{2+x}$ (1) and $Ca_{1-x}Yb_xF_{2+x}$ (2) solid solutions
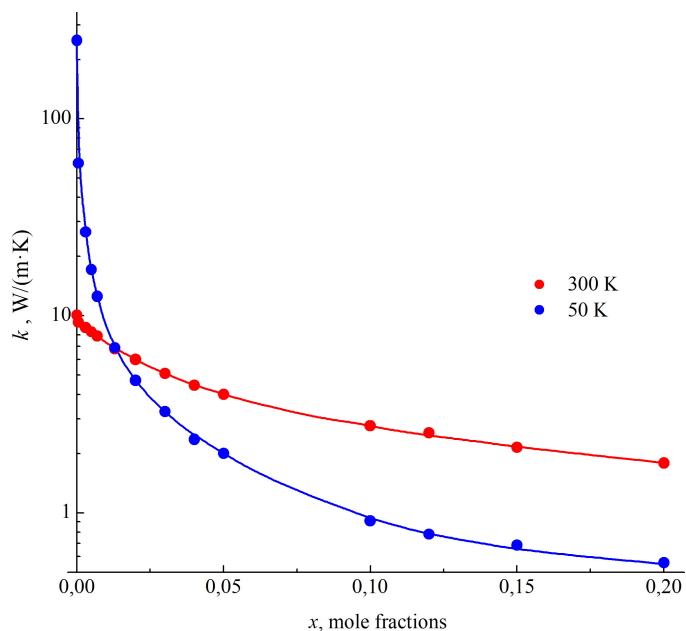


FIG. 5. Dependence of the thermal conductivity of the $Ca_{1-x}Y_xF_{2+x}$ solid solution on the content of the second component

## References

[1] Vogt T. Uber die Flusspat – Yttriumfluoritgruppe. *Neues Jahrb. Mineral*, 1914, **2** (1), P. 9–15.

[2] Sobolev B.P. *The Rare Earth Trifluorides. P. 1. The high temperature chemistry of the rare earth trifluorides*. Barcelona, Institut d'Estudis Catalans, 2000.

[3] Goldschmidt V.M., Barth T., Lunde G., Zachariasen W. *Geochemische Verteilungsgesetze der Elemente, VII, Skrift Norske Vid. Acad. Oslo, I, Mat.-Nat. Klasse*, 1926, **1** (2), S. 1–117.

[4] Bokii G.B. *Kristallokhimiya (Crystal Chemistry)*. M.: Nauka, 1971. (in Russian)

[5] Filatov S.K., Krivovichev S.V., Bubnova R.S. *Obschaya kristallokhimiya (General Crystal Chemistry)*. St. Petersburg: Izd. SPbGU, 2018. (in Russian)

[6] Hahn H., Seemann W., Kohn H.-L. Zur Mischkristallbildung in den Systemen $CaF_2$/$YF_3$, $CaF_2$/$LaF_3$, $SrF_2$/$LaF_3$ und $BaF_2$/$LaF_3$. *Zeitschrift für anorganische und allgemeine Chemie*, 1969, **369** (1–2), P. 48–58.

[7] Alexandrov V.B., Garashina L.S. New data on the structure of $CaF_2$-$TRF_3$ solid solutions. *Dokl. Akad. Nauk USSR*, 1969, **189** (2), P. 307–310. (in Russian)

[8] Fedorov P.P. , Izotova O.E., Alexandrov V.B., Sobolev B.P. New phases with fluorite-derived structure in $CaF_2$–(Y, Ln)$F_3$ systems. *J. Solid State Chem.*, 1974, **9** (4), P. 368–374.

[9] Osiko V.V., Prokhorov A.M. Investigation of the structure of crystals with an admixture of rare earth elements by spectroscopic methods. In: *Problems of modern crystallography*, M.: Nauka, 1975, P. 280–301.

[10] Cheetham A.K., Fender B.E.F., Steele D., Taylor R.I., Willis B.T.M. Defect structure of fluorite compounds containing excess anions. *Solid State Comm.*, 1970, **8**, P. 171–173.

[11] Cheetham A.K., Fender B.E.F., Cooper M.J. Defect structure of calcium fluoride containing excess anions: Bragg scattering. *J. Phys. C.: Solid State Phys.*, 1971, **4**, P. 3107–3121.

[12] Allnatt A.R., Yuen P. S. Defect interactions in ionic fluorite structures: Pair clusters in $CaF_2$ doped by $YF_3$. *J. Phys. C.: Solid State Phys.*, 1975, **8**, P. 2199–2212.

[13] Jacobs P. W.M., Ong S.H. Studies of defect clustering in $CaF_2$:$Y^{3+}$ by ionic conductivity and thermal depolarization. *J. Phys. Chem. Sol.*, 1980, **41**, P. 431–436.

[14] Laval J.P., Frit B. Defect structure of anion-excess fluorite-related $Ca_{1-x}Y_xF_{2+x}$ solid solutions. *J. Solid State Chem.*, 1983, **49**, P. 237–246.

[15] Laval J.P., Abaouz A., Frit B., Le Bail A. Short-range order in the ànion-excess fluorite-related $Ca_{0.68}Ln_{0.32}F_{2.32}$ solid solutions: EXAES study of the Eu environment. *J. of Solid State Chemistry*, 1990, **85** (1), P. 133–143.

[16] Catlow C.R.A., Chadwick A.V., Corish J., Moroney L.M., O'Reilly A.N. Defect structure of doped $CaF_2$ at high temperatures. *Phys. Rev. B*, 1989, **39** (3), P. 1897–1906.

[17] Hofmann M., Hull S., Mclntyre G.J., Wilson C.C. A neutron diffraction study of the superionic transition in $(Ca_{1-x}Y_x)F_{2+x}$. *J. Phys.: Condens. Matter.*, 1997, **9**, P. 845–857.

[18] Hull S., Wilson C.C, The defect structure of anion-excess $(Ca_{1-x}Y_x)F_{2+x}$ with $x = 0.06$. *J. Solid State Chem.*, 1992, **100** (1), P. 101–114.

[19] Wang F., Grey C.P. Probing the defect structure of anion-excess $Ca_{1-x}Y_xF_{2+x}$ ($x = 0.03 - 0.32$) with high-resolution 19 F magic-angle spinning nuclear magnetic resonance spectroscopy. *Chem. Mater.*, 1998, **10**, P. 3081–3091.

[20] Bendall P.J., Catlow C.R.A., Corish J., Jacobs P.W.M. Jacobs. Defect aggregation in anion-excess fluorites. II. Clusters containing more than two impurity atoms. *J. Solid State Chem.*, 1984, **51**, P. 159–169.

[21] Otroshchenko L.P., Aleksandrov V.B., Bydanov N.N., Simonov V.I., Sobolev B.P. Neutron diffraction refinement of the structure of the $Ca_{0.9}Y_{0.1}F_{2.1}$ solid solution. *Crystallography*, 1988, **33** (3), P. 764–765.

[22] Krahl T., Scholz G., Kemnitz E. Solid Solutions $CaF_2–YF_3$ with Fluorite Structure Prepared on the Sol–Gel Route: Investigation by Multinuclear MAS NMR Spectroscopy. *J. Phys. Chem. C*, 2014, **118** (36), P. 21066–21074.

[23] Bevan D.J.M., Greis O., Strahle J. A new structural principle in anion-excess fluorite-related superlattices. *Acta Cryst.*, 1980, **36** (6), P. 889–890.

[24] Greis O., Haschke J.M. *Rare Earth Fluorides. Handbook on the Physics and Chemistry of Rare Earth*. Ed. K.A. Gscheidner & L. Eyring. Amsterdam, New York, Oxford, 1982, **5** (45), P. 387–460.

[25] Sobolev B.P. *The Rare Earth Trifluorides. P. 2. Introduction to Materials Science of Multicomponent Metal Fluoride Crystals*. Barcelona, Institut d'Estudis Catalans, 2001.

[26] Sobolev B.P., Golubev A.M., Erero P. Fluorite phases $M_{1-x}R_xF_{2+x}$ {M – Ca, Sr, Ba; R – rare earth elements) – nanostructured materials. *Crystallography*. 2003, **48** (1), P. 148–169.

[27] Kuznetzov S.V., Osiko V.V., Tkatchenko E.A., Fedorov P.P. Inorganic nanofluorides and related nanocomposites. *Russian Chem. Rev.*, 2006, **75** (12), P. 1065–1082.

[28] Alexandrov A.A., Rezaeva A.D., Konyushkin V.A., Nakladov A.N., Kuznetsov S.V., Fedorov P.P. Features of $Ca_{1-x}Y_xF_{2+x}$ solid solution heat capacity behavior: diffuse phase transition. *Nanosystems: Physics, Chemistry, Mathematics*, 2023, **14** (2), P. 279–285.

[29] Kuznetsov S.V., Fedorov P.P. Morphological Stability of Solid-Liquid Interface during Melt Crystallization of Solid Solutions $M_{1-x}R_xF_{2+x}$. *Inorg. Mater.*, 2008, **44** (13), P. 1434–1458. (Supplement)

[30] Bagdasarov Kh.S., Voronko Yu.K., Kaminskii A.A., Krotova L.V., Osiko V.V. Modification of the optical properties of $CaF_2$-$TR^{3+}$ crystals by yttrium impurities. *Phys. stat. sol.*, 1965, **12**, P. 905–912.

[31] Iparraguirre I., Azkargorta J., Fernández J., Balda R., Oleaga A., Kaminskii A.A. Laser spectral dynamics of $Nd^{3+}$ in $CaF_2–YF_3$ crystals. *J. Optical Soc. America B*, 1999, **16** (9), P. 1439–1446.

[32] Fernández J., Oleaga A., Azkargorta J., Iparraguirre I., Balda R., Voda M., Kaminskii A.A. $Nd^{3+}$ laser spectral dynamics in $CaF_2–YF_3–NdF_3$ crystals. *Optical Materials*, 1999, **13** (1), P. 9–16.

[33] Kuznetsov S.V., Alexandrov A.A., Fedorov P.P. Optical Fluoride Nanoceramics. *Inorg. Mater.*, 2021, **57** (6), P. 555–578.

[34] Wu Y., Su L., Wang Q., Li H., Zhan Y., Jang D., Qian X., Wang C., Zheng L., Chen H., Xu J., Ryba-Romanowski W., Solarz P., Lisiecki R. Spectroscopic properties of Yb-doped $CaF_2–YF_3$ solid-solution laser crystal. *Laser Physics*, 2013, **23** (10), 105805.

[35] Su L.B., Wang Q.G., Li H.J., Brasse G., Camy P., Doualan J.L., Braud A., Moncorgé R., Zhan Y.Y., Zheng L.H., Qian X.B., Xu J. Spectroscopic properties and CW laser operation of Nd, Y-codoped $CaF_2$ single crystals. *Laser Phys. Lett.*, 2013, **10** (3), 035804.

[36] Chen H., Ikesue A., Noto H., Uehara H., Ushinuma Y., Muroga T., Yasuhara R. $Nd^{3+}$ -activated $CaF_2$ ceramic lasers. *Optics Letters*, 2019, **44** (13), P. 3378–338.

[37] Doualan J.L., Su L.B., Brasse G., Benayad A., Ménard V., Zhan Y.Y., Braud A., Camy P., Xu J., Moncorgé R. Improvement of infrared laser properties of Nd:$CaF_2$ crystals via codoping with $Y^{3+}$ and $Lu^{3+}$ buffer ions. *J. Opt. Soc. Am. B*, 2013, **30**, P. 3018–3021.

[38] Wang Q., Su L., Ma F., Zhan Y., Jiang D., Qian X., Wang J., Zheng L., Xu J., Ryba-Romanowski W., Solarz P., Lisiecki R. $Nd^{3+}$:$CaF_2$ crystal with controlled photoluminescence spectroscopic properties by codoping $Y^{3+}$ ions. *Optical Materials*, 2013, **36**, P. 455–457.

[39] Qin Z.P., Xie G.Q., Ma J., Ge W.Y., Yuan P. , Qian L.J., Su L.B., Jiang D.P., Ma F.K., Zhang Q., Cao Y.X., Xu J. Generation of 103 fs mode-locked pulses by a gain linewidth-variable Nd,Y:$CaF_2$ disordered crystal. *Optics Letters*, 2014, **39**, 1737.

[40] Li C., Fan M., Liu J., Su L., Jiang D., Qian X., Xu J. Operation of continuous wave and Q-switching on diode-pumped Nd,Y:$CaF_2$ disordered crystal. *Optics & Laser Technology*, 2015, **69**, P. 140–143.

[41] Sun Z., Mei B., Li W., Liu X., Su L. Synthesis and optical characterizations of Nd, Y:$CaF_2$ transparent ceramics. *Optical Materials*, 2017, **71**, P. 35–40.

[42] Li W., Huang H., Mei B., Song J., Xu X. Effect of $Y^{3+}$ ion doping on the microstructure, transmittance and thermal properties of $CaF_2$ transparent ceramics. *J. of Alloys and Compounds*, 2018, **747**, P. 359–365.

[43] Liu X.-Q., Hao G.-Q., Liu J., Liu D.-H., Li W.-W., Su L.-B. Yb:$CaF_2–YF_3$ transparent ceramics ultrafast laser at dual gain lines. *Chin. Phys. B*, 2022, **31** (11), 114205.

[44] Tian J., Cao X., Wang W., Liu J., Dong J., Hu D., Wang Q., Xue Y., Xu X., Xu J. Crystal growth, spectral properties and Judd-Ofelt analysis of Pr:$CaF_2–YF_3$. *Chinese Phys. B*, 2021, **30** (10), 108101.

[45] Li W., Huang H., Mei B., Wang C., Liu J., Wang Sh., Jiang D., Su L. Fabrication, microstructure and laser performance of $Yb^{3+}$ doped $CaF_2–YF_3$ transparent ceramics. *Ceramics Int.*, 2020, **46** (11), Part B, P. 19530–19536.

[46] Zhang Y., Zhao Q., Shao B., Lü W., Dong X., You H. Facile hydrothermal synthesis and luminescent properties of Eu-doped $CaF_2$–$YF_3$ alkaline-earth ternary fluoride microspheres. *RSC Advances*, 2014, **4**, P. 35750–35756.

[47] Jiang D., Zhan Y., Zhang Q., Ma F., Su L., Tang F., Qian X., Xu J. Nd,Y:$CaF_2$ Laser Crystals: Novel Spectral Properties and Laser Performance from a Controlled Local Structure. *CrystEngComm*, 2015, **17**, P. 7398–7405.

[48] Babu B.H., Billotte Th., Lyu Ch., Poumellec B., Lancry M., Hao X.-T. Study of femtosecond laser writing in the bulk of Nd, Y co-doped $CaF_2$ crystals. *OSA Continuum*, 2018, **2** (1), P. 151–161.

[49] Liu X., Yang K., Zhao S., Li T., Luan C., Guo X., Zhao B., Zheng L., Su L., Xu J., Bian J. Growth and lasing performance of a Tm, Y: $CaF_2$ crystal. *Opt. Lett.*, 2017, **42** (13), P. 2567–2570.

[50] Tian J., Cao X., Wang W., Liu J., Dong J., Hu D., Wang Q., Xue Y., Xu X., Xu J. Crystal growth, spectral properties and Judd–Ofelt analysis of Pr: $CaF_2$–$YF_3$. *Chinese Phys. B*, 2021, **30** (10), 108101.

[51] Zhu J., Zhang L., Gao Z., Wang J., Wang Zh., Su L., Zheng L., Wang J., Xu J., We Zh. Diode-pumped femtosecond mode-locked Nd, Y-codoped $CaF_2$ laser. *Laser Phys. Lett.*, 2015, **12**, 035801.

[52] Ivanov-Shitz A.K., Murin I.V. *Ionika tverdogo tela. (Solid State Ionics*. St. Petersburg: SPbU, 2010. (in Russian)

[53] Ivanov-Shits A.K., Sorokin N.I., Fedorov P.P., Sobolev B.P. Specific features of ionic transport in nonstoichiometric fluorite-type $Ca_{1-x}R_xF_{2+x}$ (R = La-Lu, Y, Sc) phases. *Solid State Ionics*, 1990, **37**, P. 125–137.

[54] Sobolev B.P., Sorokin N.I., Bolotina N.B. Nonstoichiometric single crystals $M_{1-x}R_xF_{2+x}$ and $R_{1-y}M_yF_{3-y}$ (M = Ca, Sr, Ba, R – rare earth elements) as fluorine-ionic conductive solid electrolytes. In: *Photonic and electronic properties of fluoride materials*. Ed. A. Tressaud, K. Poeppelmeier. Amsterdam e.a.: Elsevier, 2016. P. 465–491.

[55] Mogilevsky B.M., Tumpurova V.F., Chudnovsky A.F. *Eng. Phys. J.*, 1974, **27** (2), P. 287–295.

[56] Popov P.A., Fedorov P.P., Osiko V.V. Thermal Conductivity of Single Crystals of the $Ca_{1-x}Y_xF_{2+x}$ Solid Solutions. *Doklady Physics*, 2014, **59** (5), P. 199–202.

[57] Popov P.A., Shchelokov A.V., Fedorov P.P. Numerical model of temperature-dependent thermal conductivity in $M_{1-x}R_xF_{2+x}$ heterovalent solid solution nanocomposites where M stands for alkaline-earth metals and R for rare-earth metals. *Nanosystems: Phys. Chem. Math.*, 2024, **15** (2), P. 255–259.

[58] Liu K., Bian G., Zhang Z., Ma F., Su L. Modelling and analyzing the glass-like heat transfer behavior of rare-earth doped alkaline earth fluoride crystals. *CrystEngComm*, 2022, **24**, 6468.

[59] Liu K., Bian G., Zhang Z., Ma F., Su L. Simulation and demonstration of glass-like heat transfer equations in rare-earth doped alkaline earth fluoride crystals. *Chinese J. of Physics*, 2024, **88**, P. 584–593.

[60] Popov P.A., Sidorov À.À., Kul'chenkov E.A., Anishchenko A.M., Avetisov I.Sh., Sorokin N.I., Fedorov P.P. Thermal conductivity and expansion of $PbF_2$ single crystal. *Ionics*, 2017, **23** (1), P. 233–239.

[61] Popov P.A., Fedorov P.P., Reiterov V.M., Garibin E.A., Demidenko A.A., Mironov I.A., Osiko V.V. Thermal conductivity of single crystals of $Ca_{1-x}Er_xF_{2+x}$ and $Ca_{1-x}Tm_xF_{2+x}$ solid solutions. *Doklady Physics*, 2012, **57** (3), P. 97–99.

[62] Popov P.A., Fedorov P.P., Konyshkin V.A. Heat Conductivity of $Ca_{1-x}R_xF_{2+x}$ (R = La, Ce, or Pr; $0 \leq x \leq 0.25$) Heterovalent Solid Solutions. *Crystallogr. Rep.*, 2015, **60** (5), P. 744–748.

[63] *Popov P.A., Fedorov P.P. Thermal conductivity of fluoride optical materials. Bryansk: "Desyatochka" Group of Companies, 2012. (in Russian)*

[64] Gettmann W., Greis O. Uber fluorit- und tysonitverwandte ordnungsphasen im system $CaF_2$-$YF_3$. *J. Solid State Chem.*, 1978, **26** (3), P. 255–263.

[65] Greis O. Pulverrontgenographische untersuchungen und einkristal-elektronen-diffraktion an Tveitit $Ca_{13+\delta}(Y,SE)_{6-\delta}F_{44-\delta}$. *Rev. Chim. Miner.*, 1978, **15** (6), P. 481–493.

[66] Golubev A.M. *Nanometer-sized clusters in the structures of $Ba_{1-x}R_xF_{2+x}$ fluorite phases and ordered phases with a derivative structure*. Thesis. M. Schubnikov Institute of Crystallography RAS, 2009.

[67] Kazanskii S.A., Ryskin A.I., Nikiforov A.E., Zaharov A.Yu., Ougrumov M.Yu., Shakurov G.S. EPR spectra and crystal field of hexamer rare-earth clusters in fluorites. *Phys. Rev. B*, 2005, **72**, 014127.

[68] Popov P.A., Dukel'skii K.V., Mironov I.A., Smirnov A.N., Smolyanskii P.L., Fedorov P.P., Osiko V.V., Basiev T.T. Thermal conductivity of $CaF_2$ optical ceramics. *Doklady Physics*, 2007, **52** (1), P. 7–9.

*Information about the authors:*

*Pavel A. Popov* – Petrovsky Bryansk State University, 14 Bezhitskaya str., Bryansk, 241036 Russia; ORCID 0000-0001-7555-1390; tfbgubry@mail.ru

*Alexandr V. Shchelokov* – Petrovsky Bryansk State University, 14 Bezhitskaya str., Bryansk, 241036 Russia; ORCID 0009-0001-4090-2506; alexandershchelokov@mail.ru

*Vasilii A. Konyushkin* – Prokhorov General Physics Institute of the Russian Academy of Sciences, 38 Vavilova str., Moscow, 119991 Russia; ORCID 0000-0002-6028-8937; vasil@lst.gpi.ru

*Andrey N. Nakladov* – Prokhorov General Physics Institute of the Russian Academy of Sciences, 38 Vavilova str., Moscow, 119991 Russia; ORCID 0000-0002-4060-8091; andy-nak@yandex.ru

*Pavel P. Fedorov* – Prokhorov General Physics Institute of the Russian Academy of Sciences, 38 Vavilova str., Moscow, 119991 Russia; ORCID 0000-0002-2918-3926; ppfedorov@yandex.ru

*Conflict of interest*: the authors declare no conflict of interest.